Materials Research Proceedings 54 (2025) 49-58 https://doi.org/10.21741/9781644903599-6

Design of experiment on smart materials: tensile test on 3D printed composites reinforced with continuous carbon fiber and resistivity detection

Imi Ochana[1,2,a *], François Ducobu[2], Mohamed Khalil Homrani[2], and Anthonin Demarbaix[1]

[1]Science and Technology Research Unit, Haute Ecole Provinciale de Hainaut Condorcet, Boulevard Solvay 31, 6000 Charleroi, Belgium

[2] Machine Design and Production Engineering Lab, Research Institute for Science and Material Engineering, University of Mons, Mons, Belgium

[a]imi.ochana@condorcet.be

Keywords: Additive Manufacturing, Smart Materials, Design of Experiment

Abstract. Structural Health Monitoring (SHM) refers to the process of continuously assessing the condition of materials and structures to detect damage, degradation, or performance changes over time. It uses sensors integrated into materials to monitor their behavior, enabling a better understanding of aging and structural integrity, which is particularly important in industries relying on advanced manufacturing methods. The aim of this study is to investigate the integration of SHM within additive manufacturing by exploring the relationship between the mechanical and electrical properties of Continuous Carbon Fiber Reinforced Thermoplastic Polymer composites. By embedding monitoring capabilities directly into the manufacturing process, this research seeks to overcome challenges related to material performance monitoring in industrial applications. Specimens compliant with ASTM D638 were fabricated using Fused Deposition Modeling (FDM) with coextrusion technology, which exposed the reinforcing carbon fibers at their ends for resistivity measurements. Carbon fiber's electrical conductivity is leveraged to study variations in resistivity under mechanical stress. Three key variables were examined: carbon fiber filling patterns (U-shaped and W-shaped), the number of fiber layers, 2 or 4, and matrix filling densities, 10% or 30%. Tensile tests, conducted at 0.05 mm/s with a maximum tensile force of 2500 N, measured elongation, Young's modulus, resistivity and Gauge Factor (GF). The results provide critical insights into SHM integration in additive manufacturing.

Introduction

Structural Health Monitoring (SHM) refers to a set of techniques to continuously assess the condition of materials and structures to detect potential damage, signs of degradation, or changes in performance over time. This field plays a key role in preventing structural failures and optimizing the lifecycle of materials [1]. Its importance is particularly pronounced in critical sectors such as aerospace, energy, and civil infrastructure, where reliability and structural safety are paramount. In these domains, progress in advanced manufacturing, especially additive manufacturing (AM), enables the production of complex and highly customized structures but also poses challenges in ensuring their long-term integrity [2]. Recent advances in SHM technologies have significantly improved the ability to monitor the integrity of materials and structures in real-time. Modern SHM systems leverage integrated sensors, such as strain gauges, fiber optic sensors, and piezoelectric devices, to collect high-resolution data on structural behavior under various conditions [3,4]. These systems, combined with advancements in data processing and analysis, including machine learning and predictive algorithms, enable early detection of potential issues and provide actionable insights to prevent failures. Real-time monitoring capabilities are

particularly valuable in applications requiring rapid responses, such as aerospace and civil infrastructure, where safety and performance are critical [5].

Recent studies have also explored the potential of additive manufacturing, particularly Fused Deposition Modelling (FDM), for creating materials with integrated monitoring capabilities. FDM is a 3D printed method based on material extrusion for polymers and fiber-reinforced composites. Demarbaix et al. [2] investigated the use of a composite material, consisting of continuous carbon fibers as reinforcement embedded within a Polyamide (PA) matrix, in additive manufacturing via coextrusion FDM technology. They demonstrated that carbon fibers improve mechanical properties and provide electrical signals for detecting deformation and defects. The study found that fiber placement significantly affects electrical properties, with fiber-matrix adhesion being reliable during the elastic phase but less so after plastic deformation. Ryan et al. [6] investigated the use of conductive filaments in the FDM process, noting that while these materials enable electrical functionality, they often compromise mechanical performance. To address this challenge, the authors recommend combining conductive polymers with a secondary polymer to enhance both conductivity and mechanical properties, providing a balanced approach to material design. Melnykowycz et al. [7] developed carbon black/polycaprolactone (PCL) filaments as strain sensors for wearable applications, such as detecting finger motion in gloves. They found that carbon black/TPE monofilaments with a 0.3 mm diameter provided superior signal strength, precision, and stability compared to larger diameters and commercial sensors. The study concluded that these filaments are ideal for continuous strain monitoring in high-deformation wearable systems. Lopes et al. [8] studied strain-sensing in epoxy-based nanocomposites enhanced with carbon nanomaterials like reduced graphene oxide (rGO) and carbon nanofibers (CNFs). The rGO composites showed higher stability, while CNFs created new conductive pathways under strain. The study also explored integrating these nanocomposites into carbon fiber-reinforced polymers (CFRP) for structural health monitoring. While promising electrical signal variations were observed, challenges in transferring sensing capabilities due to CFRP's electrical conductivity were noted. The research highlights the potential of rGO and CNF nanocomposites for damage detection in advanced materials. Kim et al. [9] developed a method for fabricating multiaxial force sensors using dual-nozzle FDM. They combined Thermoplastic Polyurethane (TPU) for structure and carbon nanotubes for sensing. This approach allows simultaneous fabrication of both parts, eliminating extra assembly. The sensors, integrated into 3D-printed parts, detect force through resistance changes in three axes. The study highlights the impact of additive manufacturing anisotropy on signal recovery and demonstrates these sensors as a cost-effective, customizable solution for real-time force measurement. Gonçalves et al. [10] developed Polyether Ether Ketone (PEEK) based nanocomposite filaments for additive manufacturing by incorporating multi-walled carbon nanotubes (MWCNTs) and graphene nanoplatelets (GnPs). This improved electrical conductivity for FDM applications while preserving mechanical properties. The study highlighted the role of GnPs in enhancing conductivity and noted challenges in maintaining conductivity during processing. Their work demonstrates the potential of optimizing filler ratios to create advanced materials with integrated monitoring capabilities.

One promising development in AM is the use of continuous carbon fiber-reinforced thermoplastic polymers. These composites combine the flexibility and processability of thermoplastics with the exceptional strength-to-weight ratio and stiffness of carbon fibers [11]. Furthermore, the reinforcement of thermoplastics with continuous carbon fibers introduces new possibilities for designing smart materials capable of monitoring their own structural health. Such materials are highly desirable in industries where durability, safety, and performance are critical. An additional advantage of carbon fibers lies in their intrinsic electrical conductivity, which can be harnessed to enable real-time monitoring capabilities. By integrating this property into the additive manufacturing process, it becomes possible to embed SHM directly within the material

itself. This approach eliminates the need for external sensors, reducing complexity and enhancing the material's overall functionality. Combining additive manufacturing with the conductive properties of carbon fibers thus represents a significant step toward creating intelligent materials with built-in SHM capabilities. These materials can continuously provide feedback on their structural integrity, addressing challenges related to material aging and performance degradation in advanced industrial applications [8].

This study uses a Design of Experiment (DoE) which focuses on key variables such as continuous fiber filling patterns, the number of fiber layers, and matrix density. Tensile tests are conducted to determine the mechanical properties, specifically Young's modulus and yield strength (Re0.2), while the initial resistance (R_0) and gauge factor (GF) are measured under mechanical stress to evaluate the material's electrical behavior. The GF is defined in Eq. 1 as the ratio of the relative change in electrical resistance to the relative elongation:

$$GF = \frac{\frac{\Delta R}{R_0}}{\frac{\Delta L}{L_0}}, \quad (1)$$

where ΔR the change in resistance, R_0 the initial resistance (in Ω), ΔL the change in length, and L_0 (in m) is the initial length [12]. For this study, the GF is considered only in the linear portion of the strain-resistance relationship. This ensures that the calculation relies on a well-understood, stable, and reversible material behavior, which improves the reliability and accuracy of the measurements. By analyzing the interactions between these responses, the study aims to optimize both the mechanical and electrical performance of the composites, enabling the seamless integration of SHM into the additive manufacturing process.

Method

The specimens used in this study were fabricated following the ASTM D638 type I standard for tensile testing [13]. These specimens were made of continuous carbon fiber-reinforced thermoplastic composites, with a PA matrix. The fabrication process was carried out using the Anisoprint Composer A4, a 3D printer that employs FDM with coextrusion technology. This method enabled the integration of continuous carbon fibers within the PA matrix, arranged in superimposed layers to ensure continuous connectivity throughout the specimen. This arrangement allowed all fibers within each layer to be electrically connected, facilitating reliable resistivity measurements by exposing the fiber ends for electrical connectivity [14].

Each factor of the DoE was analyzed at two levels, as summarized in Table 1.

Table 1 – Studied factors of DoE, including the M320 reference configuration for baseline comparisons.

Studied factors	***Carbon fiber filling patterns***	***Carbon fiber layers***	***Density***
Low level	U	2	10%
High level	W	4	30%
Reference	M	3	20%

The carbon fiber filling patterns, illustrated in Fig. 1, were evaluated with a U pattern representing the low level and a W pattern representing the high level.

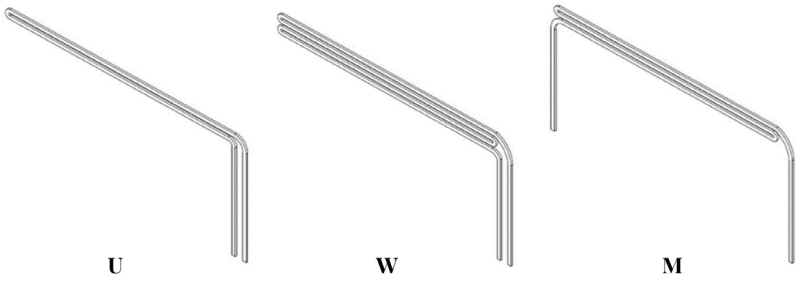

Figure 1 – Continuous carbon fiber pattern inside the specimen.

The number of carbon fiber layers varied between two, corresponding to the low level, and four, corresponding to the high level. Similarly, the matrix density was controlled at 10% for the low level and 30% for the high level. A reference specimen family, named M320, was introduced to serve as the midpoint of these studied factors. This reference configuration features three continuous carbon fiber layers arranged sequentially, with a matrix density of 20%. In this setup, each fiber path traverses three times, forming a distinctive M pattern, as shown in Fig. 1. The M320 configuration provides a balanced baseline for comparing the effects of the studied factors across their respective levels.

The variation of the studied parameters provided essential insights into their contribution to the mechanical and electrical behavior of the materials, enabling a better understanding of their potential applications in structural health monitoring and sensor technologies. The study involved eight distinct specimen families, with three identical specimens fabricated per family to ensure repeatability and statistical reliability, systematically evaluating the effects of the studied factors and their interactions.

Given that the total length of carbon fiber filament passing through each specimen remains constant, similar mechanical properties are expected for specimen families with the same total number of fiber paths. For instance, the W210 family, which contains a total of 8 carbon fiber paths with a matrix density of 10%, is anticipated to exhibit mechanical properties comparable to the U410 family, which also contains 8 fiber paths. Likewise, the W230 family and the U430 family, both containing also 8 fiber paths, should display analogous mechanical behavior. This prediction is based on the assumption that the mechanical strength and stiffness are primarily governed by the total fiber content within the specimens, regardless of the specific fiber arrangement pattern.

The tensile tests, shown in Fig. 2, were conducted to evaluate the mechanical properties of the fabricated specimens, including Young's modulus E and yield strength Re0.2. These tests were performed using a Zwick/Roëll Z2.5 universal testing machine under controlled conditions. The testing speed was set at 0.05 mm/s, and the maximum tensile force applied during the experiments was limited to 2500 N to ensure consistent measurements across all specimen configurations. Each specimen was securely clamped between the grips of the testing machine, ensuring proper alignment to prevent off-axis loading. The force was gradually applied until the specimen failed, and the resulting stress-strain data were recorded for analysis. The superimposed arrangement of the carbon fiber layers was designed to enhance the mechanical integrity of the composite and maintain connectivity between fibers across layers, ensuring uniform stress distribution. These measurements provided critical insights into the mechanical behavior of the composites under uniaxial tensile stress, helping to identify the impact of different fiber filling patterns, the number of carbon fiber layers, and matrix density on the overall performance.

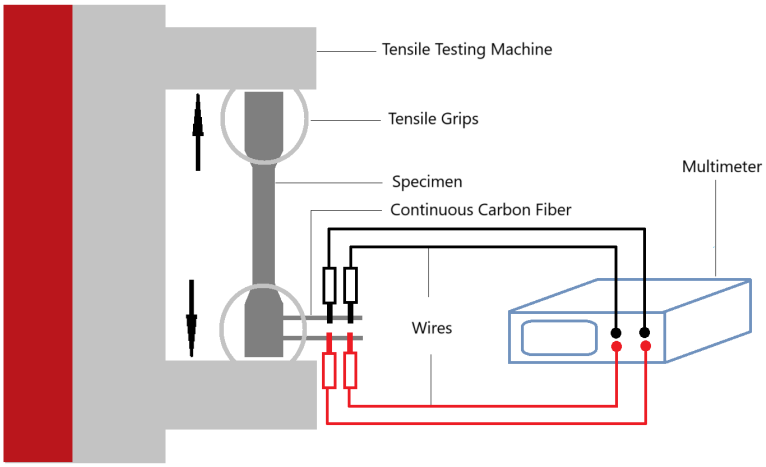

Figure 2 – Tensile test setup, showing the specimen held in the grips of the testing machine with the forces applied along its longitudinal axis.

To assess the electrical behavior of the carbon fiber-reinforced composites, resistivity measurements were conducted from the tensile tests. The exposed ends of the continuous carbon fibers in the specimens were utilized to establish electrical connections. The connectivity of the fibers across all superimposed layers ensured that resistivity measurements represented the collective contribution of all layers. Test clips were attached directly to these exposed fibers, as depicted in Fig. 3, to ensure consistent electrical contact.

Figure 3 – Electrical resistivity measurement setup, highlighting the test clips connections and the specimen.

An initial current of 1 mA was injected into the specimens using a precision power supply, while a multimeter Keithley DMM6500 was used to record the voltage drop across the fibers. From these data, the electrical resistivity was calculated for each specimen configuration. The uniform connectivity across the fiber layers allowed for accurate resistivity measurements and ensured that the electrical properties were representative of the entire composite structure. The variations in resistivity provided insight into the potential of carbon fiber composites to act as sensors for deformation and damage detection.

Results and Interpretations

The studied factors and their levels, as well as the interactions between the factors, were analyzed to evaluate their combined effects on the responses. The responses were categorized into mechanical and electrical domains. The mechanical responses included the Young's modulus E and the 0.2% offset yield strength Re0.2%, both of which provide critical information on the stiffness and strength of the composites. The electrical response focused on the initial electrical resistance R_0 and the gauge factor GF, which reflects the sensitivity of the material to deformation and is an essential parameter for strain sensing applications.

A mathematical model was established to describe the relationship between the factors and the measured responses. The factorial model for the three studied factors is expressed in Eq. 2.

$$y = a_0 + a_1x_1 + a_2x_2 + a_3x_3 + a_{12}x_1x_2 + a_{13}x_1x_3 + a_{23}x_2x_3 + a_{123}x_1x_2x_3 \quad (2)$$

In this model, *y* represents the predicted response, such as E, Re0.2%, R_0, or GF. The variables x_1, x_2, and x_3 correspond to the coded values of the studied factors, namely the carbon fiber filling patterns, the number of carbon fiber layers, and the matrix density, respectively. The parameter a_0 is the intercept, while a_1, a_2, and a_3 denote the main effects of each factor. The interaction effects between the factors are captured by the coefficients a_{12}, a_{13}, a_{23}, and a_{123}.

The coefficients of the model, as summarized in Table 2, provide valuable insights into the relative significance and direction of influence of each factor and their interactions. Positive coefficients indicate a direct relationship, where increasing the level of a factor results in an increase in the response. Conversely, negative coefficients reflect an inverse relationship.

Table 2 – Table of Effects of DoE.

Effects	a_0	a_1	a_2	a_3	a_{12}	a_{13}	a_{23}	a_{123}
E [MPa]	2514.2	268.33	329.60	28.23	-49.66	-119.55	54.58	78.81
Re0,2 [MPa]	35.50	2.870	5.228	1.218	0.748	-1.180	-0.527	0.665
R_0 [Ω]	31.70	6.35	-6.98	0.21	-2.21	0.42	-0.59	0.37
GF [/]	0.529	0.001	0.014	-0.009	-0.038	-0.011	0.015	-0.063

This model enables the prediction of material responses, such as E, Re0.2%, R_0 and GF, for any combination of factor levels without the need for additional experiments. As a result, it significantly reduces the time and effort associated with experimental testing while providing a framework for analyzing the behavior of the materials.

The tensile test experiments provided valuable insights into the mechanical and electrical responses of the specimens, as detailed in Table 3. Regarding the mechanical properties, a clear progressive increase in Young's modulus was observed, ranging from a minimum value of 1595 MPa to a maximum of 3171 MPa. This trend aligns with expectations, as the carbon fiber content and matrix density increase progressively across the specimen families. The yield strength values exhibited a standard deviation of 6.75 MPa, reflecting moderate variability across the tested specimens.

Table 3 – Mechanical and electrical responses of the tensile tests.

	U210			***U230***			***W210***			***W230***		
	1	***2***	***3***	***1***	***2***	***3***	***1***	***2***	***3***	***1***	***2***	***3***
E [MPa]	1595.17	1671.34	1817.33	2015.79	1989.90	2110.20	2755.60	2665.49	2760.81	2282.38	2187.25	2363.98
Re0,2 [MPa]	25.496	21.341	26.865	30.178	32.499	32.562	31.959	32.792	32.757	32.475	31.746	32.689
Ro [Ω]	29.99	28.36	29.78	31.85	33.06	27.72	46.29	45.94	47.00	48.01	49.36	46.97
GF[/]	0.797	0.608	0.496	/	0.700	0.928	0.509	0.464	0.586	0.642	0.603	0.490

	U410			***U430***			***W410***			***W430***		
	1	***2***	***3***	***1***	***2***	***3***	***1***	***2***	***3***	***1***	***2***	***3***
E [MPa]	2614.27	2557.50	2333.00	2844.65	2684.99	2716.37	3149.31	3019.46	2892.45	3103.58	3171.77	3038.27
Re0,2 [MPa]	40.914	35.176	31.647	39.589	35.818	39.565	45.094	42.074	45.365	50.045	39.269	44.280
Ro [Ω]	21.11	20.04	24.05	19.25	18.43	20.57	28.24	27.95	29.15	29.32	29.15	29.34
GF[/]	0.913	0.572	/	0.900	0.764	0.834	2.3193	0.092	0.351	0.944	0.230	0.244

When comparing families with the same number of carbon fiber filaments and identical matrix density within a single specimen, specific trends emerged. For instance, families W210 and U410 exhibited an average difference of 9% in their yield strength values, while families W230 and U430 demonstrated a slight average difference of 3%. These findings confirm that the arrangement of carbon fibers, whether distributed across two or four layers, has a minimal impact on the yield strength values. In terms of electrical responses, the initial resistance R_0 showed significant variation between specimen families. The lowest average R_0 value, 19 Ω, was recorded for the U430 family, whereas the W230 family displayed the highest average value of 48 Ω. This

represents an average difference of 60% for specimens with the same number of carbon fiber filaments but different distributions. The difference is explained by Pouillet's law, defined by Eq. 3, as the pathway length for the W configuration is longer than for the U configuration, leading to higher resistivity.

$$R_0 = \frac{\rho l}{S}, \tag{3}$$

where ρ is the resistivity (in Ωm), l (in m) is the length of the resistive element, and S (in m^2) is the cross-section of the resistive element.

Finally, the GF, calculated from the linear portion of the resistance-strain relationship and detailed in Table 4, along with its correlation coefficient R^2, generally exhibited high consistency with an average R^2 of 0.99 and a variation of up to 2% in most cases. However, certain anomalies, highlighted in Table 4, were observed. In the U230 family, only specimen U230.3 provided reliable measurements, with a GF of 0.92 and an R^2 of 0.96. Similarly, in the U410 family, the only coherent result was obtained for specimen U410.2, which showed a GF of 0.57 and an R^2 of 0.97. For the W410 family, a single valid result was recorded with a GF of 2.31 and an R^2 of 0.98. Lastly, for the W430 family, only one consistent value was obtained, with a GF of 0.94 and an R^2 of 0.97.

Table 4 – GF and correlation coefficients R^2 where highlighted cases indicate anomalies.

Specimen	*U210 1*	*U210 2*	*U210 3*	*U230 1*	*U230 2*	*U230 3*	*W210 1*	*W210 2*	*W210 3*	*W230 1*	*W230 2*	*W230 3*
GF	0.79	0.61	0.49	/	0.70	0.93	0.51	0.46	0.58	0.64	0.60	0.49
R^2	0.99	0.99	0.97	/	0.96	0.96	0.99	0.99	0.99	0.99	0.99	0.97

Specimen	*U410 1*	*U410 2*	*U410 3*	*U430 1*	*U430 2*	*U430 3*	*W410 1*	*W410 2*	*W410 3*	*W430 1*	*W430 2*	*W430 3*
GF	0.91	0.57	/	0.90	0.76	0.83	2.32	0.09	0.35	0.94	0.23	0.24
R^2	0.84	0.97	/	0.98	0.99	0.95	0.98	0.44	0.42	0.97	0.73	0.52

These results underscore the variability in specific specimen families and highlight the need for further analysis of these anomalies. Particular attention should be given to ensuring proper adhesion between the carbon fibers and the matrix, and post-treatment processes could be considered to improve the consistency of the results.

The following analysis examines how the studied factors influence the Young's modulus E, the 0.2% offset yield strength Re0.2, the initial electrical resistance R_0, and the gauge factor GF. The factors considered in the experiments include the carbon fiber filling patterns, the number of carbon fiber layers, and the matrix density. For each graph, the magnitude and direction of each factor's effect are determined by observing the slope of the corresponding line.

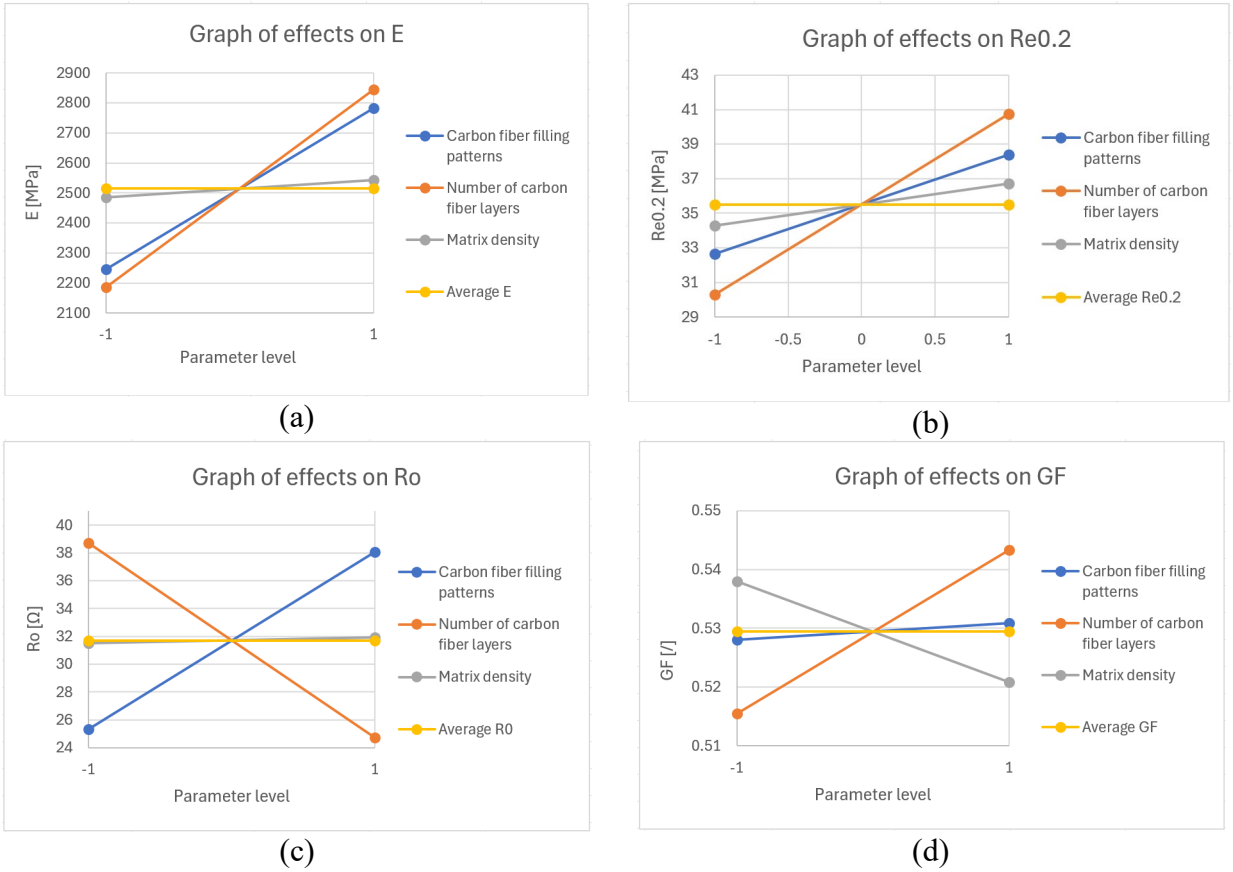

Figure 4 – (a) Graph of effects on E; (b) Graph of effects on Re 0.2; (c) Graph of effects on R_0; (d) Graph of effects on GF.

The carbon fiber filling patterns have a noticeable impact on the mechanical and electrical properties. For Young's modulus, as illustrated in Fig. 4(a), optimizing the filling patterns increases E from 2,250 MPa to 2,800 MPa, corresponding to an improvement of 23%. Similarly, as shown in Fig. 4(b), the yield strength increases from 33 MPa to 38.5 MPa, representing a 16% gain. For the initial electrical resistance, Fig. 4(c) shows that changes in filling patterns cause an increase from 25 Ω to 38 Ω, reflecting a significant rise of 35%. However, for the gauge factor, Fig. 4(d) reveals only a minimal increase from 0.529 to 0.531, which corresponds to a negligible improvement of 0.3%.

The number of carbon fiber layers has the most pronounced influence across all properties. As shown in Fig. 4(a), increasing the fiber layers raises Young's modulus from 2,200 MPa to 2,850 MPa, which corresponds to a substantial enhancement of 23%. For yield strength, as illustrated in Fig. 4(b), this parameter increases Re0.2 from 30 MPa to 41 MPa, representing an improvement of 27%. Regarding the initial electrical resistance, Fig. 4(c) shows a significant reduction from 39Ω to 25 Ω, corresponding to a decrease of 36%. For the gauge factor, as seen in Fig. 4(d), the increase is moderate, from 0.515 to 0.545, reflecting a small gain of 5.5%.

The matrix density has a comparatively smaller effect on the composite's properties. For Young's modulus, as illustrated in Fig. 4(a), E increases only slightly, from 2,450 MPa to 2,500 MPa, representing a modest gain of 2%. A similar trend is observed for yield strength, as shown in Fig. 4(b), where Re0.2 increases from 34.5 MPa to 37 MPa, reflecting a modest improvement of 7%. For the initial electrical resistance, Fig. 4(c) reveals that the matrix density has a negligible impact, with R_0 increasing marginally from 31.5 Ω to 32 Ω, representing a very small change of

1.6%. Interestingly, for the gauge factor, Fig. 4(d) shows a decrease from 0.538 to 0.520, corresponding to a reduction of 3.4%.

The objective of this experimental plan is to identify the optimal combination of factors to achieve a composite material that balances mechanical and electrical performance. Carbon fiber filling patterns and the number of fiber layers emerge as the key factors influencing the composite's properties. The filling patterns primarily affect mechanical strength and electrical resistance, while the fiber layers exhibit a dominant impact across all parameters, particularly in enhancing stiffness and reducing resistance. In contrast, matrix density plays a minor role, with limited influence on most properties except for a slight negative impact on the gauge factor.

Conclusions

This study explored the integration of SHM into additive manufacturing by analyzing the mechanical and electrical behavior of continuous carbon fiber-reinforced thermoplastic composites. The results demonstrate that the number of fiber layers is the most influential factor, leading to significant improvements in mechanical performance, including a 23% increase in Young's modulus and a 27% rise in yield strength. The fiber filling patterns (U-shaped and W-shaped) also contributed positively, though to a lesser extent, while the matrix density showed negligible influence on stiffness and strength.

In terms of electrical responses, the U-shaped filling pattern produced lower initial resistance R_0 compared to the W-shaped configuration, consistent with shorter conductive pathways. Adding more fiber layers further reduced R_0 by 36%, underscoring the importance of fiber quantity in enhancing electrical conductivity. While the GF displayed slight improvements with increasing fiber layers, matrix density had a small but negative effect. Variability and anomalies observed in certain specimen families highlight the need for further optimization of the manufacturing process to ensure consistent and reliable measurements.

In conclusion, this study confirms that optimizing the fiber quantity and arrangement is key to improving both the mechanical and electrical properties of carbon fiber composites, paving the way for the effective integration of SHM in additive manufacturing. Future work will focus on addressing observed inconsistencies and expanding the scope of SHM applications to improve material performance monitoring in industrial settings.

Acknowledgments

The authors would like to thank Région Wallonne for supporting this research as part of the SKYWIN ICOM2C3D research project under grant 8820.

References

[1] S. Metaxa, K. Kalkanis, C. S. Psomopoulos, S. D. Kaminaris, and G. Ioannidis, "A review of structural health monitoring methods for composite materials," in *Procedia Structural Integrity*, Elsevier B.V., 2019, pp. 369–375. https://doi.org/10.1016/j.prostr.2020.01.046

[2] A. Demarbaix, I. Ochana, J. Levrie, I. Coutinho, S. S. Cunha, and M. Moonens, "Additively Manufactured Multifunctional Composite Parts with the Help of Coextrusion Continuous Carbon Fiber: Study of Feasibility to Print Self-Sensing without Doped Raw Material," *Journal of Composites Science*, vol. 7, no. 9, p. 355, Aug. 2023. https://doi.org/10.3390/jcs7090355

[3] S. Nauman, "Piezoresistive Sensing Approaches for Structural Health Monitoring of Polymer Composites—A Review," Jun. 01, 2021, *Multidisciplinary Digital Publishing Institute (MDPI)*. https://doi.org/10.3390/eng2020013

[4] A. M. L. Lanzolla, F. Attivissimo, G. Percoco, M. A. Ragolia, G. Stano, and A. Di Nisio, "Additive Manufacturing for Sensors: Piezoresistive Strain Gauge with Temperature

Compensation," *Applied Sciences (Switzerland)*, vol. 12, no. 17, Sep. 2022. https://doi.org/10.3390/app12178607

[5] I. Y. Lee, J. Jang, and Y. Bin Park, "Advanced structural health monitoring in carbon fiber-reinforced plastic using real-time self-sensing data and convolutional neural network architectures," *Mater Des*, vol. 224, Dec. 2022. https://doi.org/10.1016/j.matdes.2022.111348

[6] K. R. Ryan, M. P. Down, N. J. Hurst, E. M. Keefe, and C. E. Banks, "Additive manufacturing (3D printing) of electrically conductive polymers and polymer nanocomposites and their applications," Jul. 01, 2022, *Elsevier B.V.* https://doi.org/10.1016/j.esci.2022.07.003

[7] M. Melnykowycz, B. Koll, D. Scharf, and F. Clemens, "Comparison of piezoresistive monofilament polymer sensors," *Sensors (Switzerland)*, vol. 14, no. 1, pp. 1278–1294, Jan. 2014. https://doi.org/10.3390/s140101278

[8] C. Lopes *et al.*, "Smart Carbon Fiber-Reinforced Polymer Composites for Damage Sensing and On-Line Structural Health Monitoring Applications," *Polymers (Basel)*, vol. 16, no. 19, p. 2698, Sep. 2024. https://doi.org/10.3390/polym16192698

[9] K. Kim, J. Park, J. hoon Suh, M. Kim, Y. Jeong, and I. Park, "3D printing of multiaxial force sensors using carbon nanotube (CNT)/thermoplastic polyurethane (TPU) filaments," *Sens Actuators A Phys*, vol. 263, pp. 493–500, Aug. 2017. https://doi.org/10.1016/j.sna.2017.07.020

[10] J. Gonçalves *et al.*, "Electrically conductive polyetheretherketone nanocomposite filaments: From production to fused deposition modeling," *Polymers (Basel)*, vol. 10, no. 8, Aug. 2018. https://doi.org/10.3390/polym10080925

[11] C. Pandelidi, S. Bateman, S. Piegert, R. Hoehner, I. Kelbassa, and M. Brandt, "The technology of continuous fibre-reinforced polymers: a review on extrusion additive manufacturing methods," *The International Journal of Advanced Manufacturing Technology*, 2021. https://doi.org/10.1007/s00170-021-06837-6

[12] X. Yao, C. Luan, D. Zhang, L. Lan, and J. Fu, "Evaluation of carbon fiber-embedded 3D printed structures for strengthening and structural-health monitoring," *Mater Des*, vol. 114, pp. 424–432, Jan. 2017. https://doi.org/10.1016/j.matdes.2016.10.078

[13] ASTM D638, "Standard Test Method for Tensile Properties of Plastics 1". https://doi.org/10.1520/D0638-14

[14] Read on https://anisoprint.com/ the 28th July 2024.